

Analysis of alterations in white matter integrity of adult patients with comitant exotropia

Journal of International Medical Research

2018, Vol. 46(5) 1963–1972

© The Author(s) 2018

Reprints and permissions:

sagepub.co.uk/journalsPermissions.nav

DOI: 10.1177/0300060518763704

journals.sagepub.com/home/imr



Dan Li , Shenghong Li and Xianjun Zeng

Abstract

Objective: This study was performed to investigate structural abnormalities of the white matter in patients with comitant exotropia using the tract-based spatial statistics (TBSS) method.

Methods: Diffusion tensor imaging data from magnetic resonance images of the brain were collected from 20 patients with comitant exotropia and 20 age- and sex-matched healthy controls. The FMRIB Software Library was used to compute the diffusion measures, including fractional anisotropy (FA), mean diffusivity (MD), axial diffusivity (AD), and radial diffusivity (RD). These measures were obtained using voxel-wise statistics with threshold-free cluster enhancement.

Results: The FA values in the right inferior fronto-occipital fasciculus (IFO) and right inferior longitudinal fasciculus were significantly higher and the RD values in the bilateral IFO, forceps minor, left anterior corona radiata, and left anterior thalamic radiation were significantly lower in the comitant exotropia group than in the healthy controls. No significant differences in the MD or AD values were found between the two groups.

Conclusions: Alterations in FA and RD values may indicate the underlying neuropathologic mechanism of comitant exotropia. The TBSS method can be a useful tool to investigate neuronal tract participation in patients with this disease.

Keywords

Diffusion tensor imaging, tract-based spatial statistics, magnetic resonance imaging, strabismus, comitant exotropia, white matter

Date received: 14 January 2018; accepted: 15 February 2018

Department of Radiology, The First Affiliated Hospital of Nanchang University, Nanchang, Jiangxi Province, China

Corresponding author:

Xianjun Zeng, Department of Radiology, The First Affiliated Hospital of Nanchang University, No. 17 Yongwaizheng Street, Nanchang, Jiangxi Province 330006, China.

Email: xianjun-zeng@126.com



Creative Commons Non Commercial CC BY-NC: This article is distributed under the terms of the Creative Commons Attribution-NonCommercial 4.0 License (<http://www.creativecommons.org/licenses/by-nc/4.0/>)

which permits non-commercial use, reproduction and distribution of the work without further permission provided the original work is attributed as specified on the SAGE and Open Access pages (<https://us.sagepub.com/en-us/nam/open-access-at-sage>).

Introduction

Strabismus is a disorder of ocular misalignment and has a high incidence worldwide.¹ The concomitance of deviations is used to define strabismus. Comitant exotropia is a common type of strabismus; it is characterized by a constant angle of deviation of gazing in all directions and may affect 1.0% to 4.2% of the population.² Clinically, exotropia is usually coupled with amblyopia and loss of binocular function.^{3,4} Therefore, patients with exotropia experience daily inconveniences and a negative impact on life. Surgery is generally performed for the treatment of exotropia. However, stereopsis does not recover in a proportion of adult patients who experience long-term illness after undergoing surgical treatment of exotropia.⁵ We speculate that the microstructure of the brain of patients with exotropia undergoes rearrangement, although little is known about the details of the pathogenesis.

As a noninvasive nerve imaging technique, magnetic resonance imaging (MRI), including functional MRI and structural MRI, has progressed rapidly in recent years. This technique was introduced by researchers to study the functional and structural changes in the brains of patients with strabismus. Some researchers have used MRI techniques to show alterations in brain plasticity during the early stages of visual abnormalities.^{6,7} A previous study showed that patients with strabismus demonstrate suppression of cortical activity modulations, especially in the primary visual cortex.⁸ Previous studies have only focused on the morphological changes in the strabismus-associated brain regions. We propose that alterations exist not only at the level of blood oxygenation level-dependent signals but also at the level of fasciculi.

Diffusion tensor imaging (DTI) is a sensitive sequence that reacts to the diffusivity of water⁹ and is thus a useful tool to

observe brain maturation in vivo.¹⁰ Different modes can be utilized to compute the diffusion data. Huang et al.¹¹ applied statistical parametric mapping and found that the mean diffusivity (MD) was increased in the middle frontal gyrus and anterior cingulate in patients with strabismus. In addition, Ouyang et al.¹² applied voxel-based morphometry and reported that the white matter volume was mainly decreased in the bilateral temporal gyrus, while the gray matter volume was mainly decreased in the frontal and cingulate areas in patients with strabismus. Tract-based spatial statistics (TBSS), which combines the strengths of both voxel-wise and tractography-based analyses, is widely used to investigate neurological disorders.¹³ Here, we used TBSS to study the diffusivity of fiber bundles in patients with comitant exotropia and identify changes in the nerve microstructure.

Methods

Participants

Adult patients with comitant exotropia were recruited from the Ophthalmology Department of the First Affiliated Hospital of Nanchang University in China for this study. This study was approved by the Human Research Ethics Committee of the First Affiliated Hospital of Nanchang University. All methods were performed in accordance with the relevant guidelines and regulations specified by this committee. Each participant provided written informed consent. The inclusion criteria for the patients with exotropia were as follows: an uncorrected or corrected visual acuity of >1.0 , equal angles of deviation in the strabismic group, and stereovision defects (no visual fusion). The exclusion criteria for the patients with exotropia were as follows: other types of strabismus, such as incomitant and concealed oblique strabismus;

other ophthalmic diseases; a medical history of eye treatment; psychiatric disorders or drug addiction; and MRI contraindications. All patients underwent detailed eye examinations. Additionally, age- and sex-matched healthy controls (HCs) were recruited from similar geographical areas and ethnic populations. All HCs met the following criteria: ability to undergo MRI scanning, no ophthalmic disorders, and no brain abnormalities according to the MRI examination.

Data acquisition

All MRI data were collected with a 3.0-T MRI scanner (Siemens, Erlangen, Germany) equipped with an 8-channel phased-array head coil at the Department of Radiology of the First Affiliated Hospital, Nanchang University, China. A three-dimensional T1-weighted magnetization prepared rapid acquisition gradient echo (MPRAGE) scan and a DTI spin echo planar scan were included in the data acquisition for this study. The parameters for those sequences were as follows:

T1-weighted images: repetition time (TR) = 1900 ms, echo time (TE) = 2.26 ms, flip angle = 9° , field of view (FOV) = 240×240 mm, matrix = 256×256 , slice thickness = 1 mm, and number of sagittal slices = 176.

DTI spin echo planar images: voxel size = $1 \times 1 \times 1$ mm³, TR = 8000 ms, TE = 89 ms, FOV = 250×250 mm, slice thickness = 2 mm, number of slices = 62, orientation = axial, 64 nonlinear diffusion weighting gradient directions with $b = 1000$ s/mm², and an additional b_0 (b value = 0) image.

Data preprocessing

All MRI data were preprocessed using the FMRIB Software Library (FSL) (<http://www.fmrib.ox.ac.uk/fsl>). First, all original

data were processed for brain extraction. Next, the v3.0 FMRIB Diffusion Toolbox (FDT) (<http://fsl.fmrib.ox.ac.uk/fsl/fslwiki/FDT>) was used to correct for eddy current distortion and head motion artifacts. A brain mask was then created using the script BET based on the b_0 image. Diffusion scalar measures, including fractional anisotropy (FA), MD, axial diffusivity (AD), and radial diffusivity (RD), were calculated by reconstructing a tensor matrix from the raw diffusion data using the v3.0 FDT (<http://fsl.fmrib.ox.ac.uk/fsl/fslwiki/FDT>) in the FSL.

TBSS procedures

The following data processing technique was performed to analyze the white matter diffusion properties, as described in a previous report of the TBSS approach.¹⁴ TBSS analysis was conducted separately for FA, MD, and RD, although the white matter skeleton was generated based on FA maps. All FA images were aligned to a Montreal Neurological Institute 152 (MNI152) standard space ($1 \times 1 \times 1$ mm³) through nonlinear registration, in which the FMRIB58_FA standard-space image (http://fsl.fmrib.ox.ac.uk/fsl/fslwiki/FMRIB58_FA) was regarded as the template. To create a mean FA skeleton, the mean FA maps of all participants were projected onto the FMRIB58_skeleton. The FA threshold was set at 0.2 to include major fasciculi and eliminate peripheral tracts in the case of interference of inter-subject variability or partial volume effects. To achieve nonlinear registration and skeletonization, MD, AD, and RD were respectively projected onto the original mean FA skeleton obtained from the FA registration. After full alignment with the common skeleton, the data were in the form of a four-dimensional image. The Johns Hopkins University (JHU) white-matter tractography atlas and the JHU International Consortium of Brain Mapping

Table 1. Demographic and clinical characteristics of patients with CE and HCs

	CE	HCs	t	p-value
Sex, male/female	10/10	10/10	N/A	>0.99
Age, years	32.45 ± 6.93	32.68 ± 5.23	0.019	0.987
Duration of strabismus, years	28.10 ± 9.18	N/A	N/A	N/A
Age at onset, years	4.35 ± 4.48	N/A	N/A	N/A
Best-corrected VA, right	1.07 ± 0.47	1.11 ± 0.13	-0.379	0.785
Best-corrected VA, left	1.05 ± 0.38	1.10 ± 0.26	-0.450	0.545

Data are presented as n or mean ± standard deviation. CE, comitant exotropia; HCs, healthy controls; N/A, no data; VA, visual acuity (presented as the mean of binocular values).

(ICBM)-DTI-81 white-matter labels were utilized to identify specific fiber tracts. The FSLview (v3.2.0) enabled visualization of the resulting statistical maps for those diffusion scalar measures. The statistically significant voxel clusters of FA, MD, AD, and RD were then extracted using the FSL cluster tool. The script `tbss_fill` was utilized to fill the tracts and thus visualize the representation of the actual analysis more easily.

Statistical analysis

To compare the demographic and clinical parameters between two groups, IBM SPSS Statistics, version 23.0 (IBM Corp., Armonk, NY, USA) was used with two-independent-sample t-tests ($p < 0.05$). The permutation-based nonparametric approach was conducted in our statistical analysis using the Threshold-Free Cluster Enhancement option in the FSL randomize tool. The random permutation was set at 5000 with age and sex as covariates. A level of $p < 0.05$ indicated statistical significance, which was fully corrected for multiple comparisons.

Results

Twenty adult patients with comitant exotropia (10 men, 10 women; mean age, 32.45 ± 6.93 years) and 20 age- and sex-matched HCs (10 men, 10 women; mean age, 32.68 ± 5.23 years) were included in

this study. There were no significant differences in age, sex distribution, or visual acuity between the patients and HCs, as shown in Table 1. Voxel clusters that were significantly different between the two groups were found in FA and RD. The patients showed significantly higher FA values in two clusters, including the right inferior fronto-occipital fasciculus (IFO) and the right inferior longitudinal fasciculus (ILF), compared with the HCs ($p < 0.05$) (Table 2 and Figure 1). The patients showed significantly lower RD values in six clusters, which were located in the bilateral IFO, forceps minor, left anterior corona radiata, and left anterior thalamic radiation, compared with the HCs ($p < 0.05$) (Table 3 and Figure 2). However, no significant differences in the MD or AD values were found between the two groups.

Discussion

The present study is the first TBSS analysis performed in adult patients with longstanding comitant exotropia. We compared the fiber bundle architecture between patients with comitant exotropia and HCs using DTI scanning and TBSS analysis. Briefly, our main findings were as follows. Among voxel clusters that exhibited significant differences, patients with comitant exotropia demonstrated a higher FA and lower RD than those in the HCs, whereas MD and

Table 2. Clusters showing significant differences in FA between patients with CE and HCs

Variable	Comparison	TFCE/FWE-corrected p	Cluster number	MNI atlas coordinates (mm)			Tract(s) within clusters
				X	Y	Z	
FA	HCs < CE	<0.05	1	18	-57	36	Inferior fronto-occipital fasciculus (right)
	HCs < CE	<0.05	2	40	-43	-7	Inferior longitudinal fasciculus (right)

FA, fractional anisotropy; CE, comitant exotropia; HCs, healthy controls; TFCE FWE-corrected p , Threshold-Free Cluster Enhancement family-wise error-corrected p value; MNI, Montreal Neurological Institute.

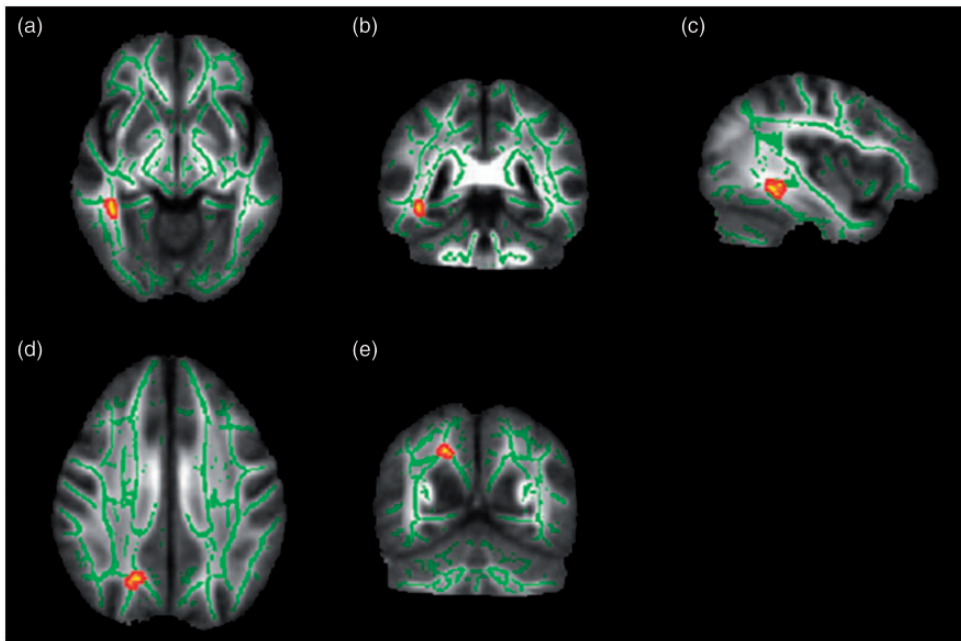


Figure 1. Results of whole-brain tract-based spatial statistics analysis comparing fractional anisotropy between patients with comitant exotropia and healthy controls. Significantly higher fractional anisotropy values were shown in the right inferior fronto-occipital fasciculus and the right inferior longitudinal fasciculus ($p < 0.05$). Parts (a)–(e) show these two clusters in different orientations.

AD were not significantly different between the two groups.

As proposed in a previous study, the TBSS approach is more robust and sensitive than other voxel-wise analytical protocols.¹⁴ The TBSS approach avoids the disadvantages of the statistical parametric

mapping-based approach, including registration and diffusion data smoothing.¹⁵ Furthermore, TBSS does not require the user to ensure that the cross-subject FA values are in concordance with the Gaussian distribution. Our study showed increased FA values in the IFO and ILF.

Table 3. Clusters showing significant differences in RD between patients with CE and HCs

Variable	Comparison	TFCEFWE-corrected <i>p</i>	Cluster number	MNI atlas coordinates (mm)			Tract(s) within clusters
				X	Y	Z	
RD	HCs > CE	<0.05	1	40	-42	-7	Inferior fronto-occipital fasciculus (right)
	HCs > CE	<0.05	2	-35	-53	-3	Inferior fronto-occipital fasciculus (left)
	HCs > CE	<0.05	3	21	41	7	Forceps minor
	HCs > CE	<0.05	4	-5	25	13	Forceps minor
	HCs > CE	<0.05	5	-23	20	28	Anterior corona radiate (left)
	HCs > CE	<0.05	6	-22	-56	25	Anterior thalamic radiation (left)

RD, radial diffusivity; CE, comitant exotropia; HCs, healthy controls; TFCE FWE-corrected *p*, Threshold-Free Cluster Enhancement family-wise error-corrected *p* value; MNI, Montreal Neurological Institute.

A voxel-based morphometric analysis in patients with strabismus was used to confirm the increased thickness of cortical regions connected via the ILF, such as the frontal gyrus.¹⁶ Similarly, in previous voxel-wise studies, FA values were increased in the medial frontal gyrus of patients with comitant exotropia.¹¹ The voxel-wise degree centrality in the temporal gyrus was increased in a study of the functional brain activity network.¹⁷ Given that the ILF is not only the major association pathway that links the occipital cortex with the temporal lobe (an indirect pathway is also linked to the frontal lobe),¹⁸ we speculate that this phenomenon might indicate more numerous dense connections or less branching within fiber bundles, representing the underlying neuropathologic mechanism. Increased FA in the IFO was an unexpected finding in our patients with comitant exotropia, which is characterized by integrity of the fiber bundles. Unlike in patients with bipolar disorder¹⁹ and Alzheimer's disease,²⁰ the FA values in the IFO were increased in the patients in our study. This might be attributed to less fiber branching and more myelination, which we believe do

not typically occur in patients with visual disorders. Inconsistent with our results, a previous study showed no significant changes in the FA values of patients with strabismic amblyopia.²¹ Likewise, previous investigators have also found that FA values were decreased in the IFO.¹¹ The IFO connects the frontal and occipital lobes along with the lateral border of the caudate nucleus. The IFO is thought to be vital for integrating information among these remote brain regions.²² A study focusing on IFO damage highlighted the significant role of this tract, which was shown to strengthen the connections between visual processing and emotion-related cortical regions, such as the connection of the visual cortex to the orbitofrontal cortex.²³ It is possible that increased FA, as in our study, might indicate well-myelinated white matter tracts, which may reflect a potential neural compensation mechanism that can serve as a biomarker for this disease.

FA can be divided into axial and radial components that represent the directionality of the diffusion tensor.²⁴ A decrease in RD was interpreted as a decrease in neuronal branching.²⁵ In our group of patients

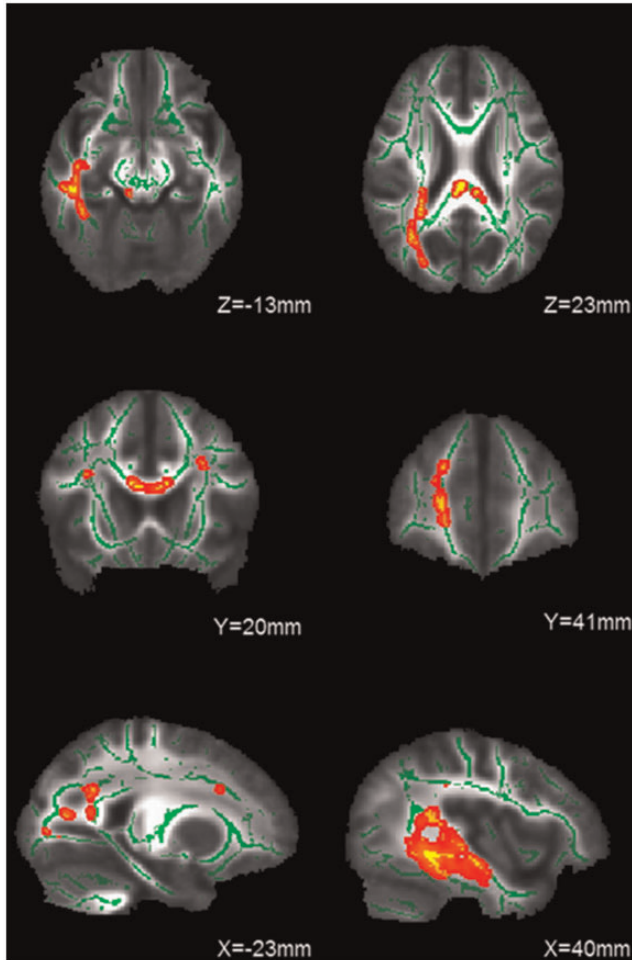


Figure 2. Comparison of radial diffusivity (RD) in patients with comitant exotropia and healthy controls. The skeleton image (green = $RD > 0.2$) was overlaid by the mean fractional anisotropy image. The yellow and red areas indicate all tracts with significantly decreased RD values in the patient group, which may reflect abnormal white matter integrity ($p < 0.05$). The statistically significant clusters are presented at different coordinates in these six parts. These clusters include the bilateral fronto-occipital fasciculus, forceps minor, left anterior corona radiata, and left anterior thalamic radiation.

with comitant exotropia, the RD values were decreased in the IFO, forceps minor, anterior corona radiata, and anterior thalamic radiation. The forceps minor consists of a lateral expansion of fibers of the corpus callosum,²⁶ which connects the dorsolateral prefrontal cortices including parts of the middle and superior frontal gyrus.²⁷ A functional MRI study indicated decreased

brain activation of the frontal gyrus in patients with infantile strabismus.²⁸ Increased FA values in the frontal gyrus and smaller white matter volumes in the middle frontal gyrus were detected in a previous study of patients with comitant exotropia.² The anterior corona radiata, part of the limbic-thalamo-cortical circuitry, contains the thalamic projections from

the internal capsule to the prefrontal cortex, which consists of the dorsolateral prefrontal cortex and the ventrolateral prefrontal cortex²⁹ and carries nearly all of the neural links to and from the cerebral cortex. Decreased gray matter density in the middle frontal gyrus was found in children with strabismic amblyopia.³⁰ A previous study demonstrated that blood oxygenation level-dependent signals of the cerebral thalamus and frontal gyrus were activated when viewing with a strabismic amblyopic eye.³¹ The anterior thalamic radiation interacts with the medial forebrain bundle to connect the thalamus with the prefrontal cortex and occipital cortex, which can control the expression of emotions through a reward-punishment circuit to achieve a dynamic balance between positive and negative emotional states.^{32,33} Previous studies have indicated that patients with strabismus experience long-term negative emotions and can obtain significant improvements in their psychosocial quality of life after undergoing strabismus surgery.^{34,35} We speculatively suggest that the decreased RD values in several tracts, as seen in our study, may reveal the neuropathologic mechanism of comitant exotropia, which attempts to compensate for impairment of neuronal tracts by reducing neuronal branching. Moreover, we speculate that those fasciculi with increased FA values and decreased RD values in patients with exotropia have a more dense alignment and less neuron branching to improve the function they handle; furthermore, the connections among those fiber bundles are weakened. Hence, our study may help to elucidate the causes of negative emotions at the microstructural level of the whole brain in patients with comitant exotropia. Moreover, we found that the microstructure of the white matter changed under the condition of drug addiction³⁶ or medication overuse.³⁷ No study to date has shown that the normal use of everyday

medication can affect the integrity of the white matter. Therefore, we did not include daily medication use as an exclusion criterion.

Finally, this study has two main limitations. First, we mainly focused on long-duration comitant exotropia. Little is known about the connections between illness duration and alterations in the white matter. Future studies are needed to elucidate this relationship. Second, we mainly investigated the diffusivities separately. We will further study how the FA and RA values impact each other.

Conclusion

This is the first TBSS analysis conducted in adult patients with longstanding comitant exotropia. The current results demonstrated the abnormalities of the tracts, which may represent the neuropathologic mechanism and the possibility of a neural compensation mechanism in patients with comitant exotropia. Overall, the TBSS method, which is a serviceably voxel-wise analytical approach, can be regarded as an indicator for auxiliary judgment of the severity of potential brain damage in patients with comitant exotropia.

Declaration of conflicting interest

The authors declare that there is no conflict of interest.

Funding

This study was supported by the National Natural Science Foundation of China (Grant No. 81760307). The funders had no role in the study design, data collection and analysis, decision to publish, or preparation of the manuscript.

ORCID iD

Dan Li  <http://orcid.org/0000-0002-0185-9234>

References

1. Gunton KB, Wasserman BN and DeBenedictis C. Strabismus. *Prim Care* 2015; 42: 393–407.
2. Yan X, Lin X, Wang Q, et al. Dorsal visual pathway changes in patients with comitant exotropia. *PLoS One* 2010; 5: e10931.
3. Bui Quoc E and Milleret C. Origins of strabismus and loss of binocular vision. *Front Integr Neurosci* 2014; 8: 71.
4. Yekta A, Hashemi H, Norouzirad R, et al. The prevalence of amblyopia, strabismus, and ptosis in schoolchildren of Dezful. *Eur J Ophthalmol* 2016; 27: 109–112.
5. Miller JM, Scott AB, Danh KK, et al. Bupivacaine injection remodels extraocular muscles and corrects comitant strabismus. *Ophthalmology* 2013; 120: 2733–2740.
6. Li Q, Bai J, Zhang J, et al. Assessment of cortical dysfunction in patients with intermittent exotropia: an fMRI study. *PLoS One* 2016; 11: e0160806.
7. Yang X, Zhang J, Lang L, et al. Assessment of cortical dysfunction in infantile esotropia using fMRI. *Eur J Ophthalmol* 2014; 24: 409–416.
8. Chen VJ and Tarczy-Hornoch K. Functional magnetic resonance imaging of binocular interactions in visual cortex in strabismus. *J Pediatr Ophthalmol Strabismus* 2011; 48: 366–374.
9. Le Bihan D. Looking into the functional architecture of the brain with diffusion MRI. *Nat Rev Neurosci* 2003; 4: 469–480.
10. Chan KC, Kancherla S, Fan SJ, et al. Long-term effects of neonatal hypoxia-ischemia on structural and physiological integrity of the eye and visual pathway by multimodal MRI. *Invest Ophthalmol Vis Sci* 2014; 56: 1–9.
11. Huang X, Li HJ, Zhang Y, et al. Microstructural changes of the whole brain in patients with comitant strabismus: evidence from a diffusion tensor imaging study. *Neuropsychiatr Dis Treat* 2016; 12: 2007–2014.
12. Ouyang J, Yang L, Huang X, et al. The atrophy of white and gray matter volume in patients with comitant strabismus: Evidence from a voxel-based morphometry study. *Mol Med Rep* 2017; 16: 3276–3282.
13. Govindan RM, Behen ME, Helder E, et al. Altered water diffusivity in cortical association tracts in children with early deprivation identified with Tract-Based Spatial Statistics (TBSS). *Cereb Cortex* 2010; 20: 561–569.
14. Smith SM, Jenkinson M, Johansen-Berg H, et al. Tract-based spatial statistics: voxelwise analysis of multi-subject diffusion data. *Neuroimage* 2006; 31: 1487–1505.
15. Abe O, Takao H, Gono W, et al. Voxel-based analysis of the diffusion tensor. *Neuroradiology* 2010; 52: 699–710.
16. Chan ST, Tang KW, Lam KC, et al. Neuroanatomy of adult strabismus: a voxel-based morphometric analysis of magnetic resonance structural scans. *Neuroimage* 2004; 22: 986–994.
17. Tan G, Dan ZR, Zhang Y, et al. Altered brain network centrality in patients with adult comitant exotropia strabismus: A resting-state fMRI study. *J Int Med Res* 2018; 46: 392–402.
18. Tendolkar I, Martensson J, Kuhn S, et al. Physical neglect during childhood alters white matter connectivity in healthy young males. *Hum Brain Mapp* 2018; 39: 1283–1290.
19. Lin F, Weng S, Xie B, et al. Abnormal frontal cortex white matter connections in bipolar disorder: a DTI tractography study. *J Affect Disord* 2011; 131: 299–306.
20. Douaud G, Jbabdi S, Behrens TE, et al. DTI measures in crossing-fibre areas: increased diffusion anisotropy reveals early white matter alteration in MCI and mild Alzheimer's disease. *Neuroimage* 2011; 55: 880–890.
21. Allen B, Spiegel DP, Thompson B, et al. Altered white matter in early visual pathways of humans with amblyopia. *Vision Res* 2015; 114: 48–55.
22. Sarubbo S, De Benedictis A, Maldonado IL, Basso G, Duffau H. Frontal terminations for the inferior fronto-occipital fascicle: anatomical dissection, DTI study and functional considerations on a multi-component bundle. *Brain Struct Funct* 2013; 218: 21–37.
23. Philippi CL, Mehta S, Grabowski T, et al. Damage to association fiber tracts impairs recognition of the facial expression of emotion. *J Neurosci* 2009; 29: 15089–15099.
24. Bode MK, Lindholm P, Kiviniemi V, et al. DTI abnormalities in adults with past

- history of attention deficit hyperactivity disorder: a tract-based spatial statistics study. *Acta Radiol* 2015; 56: 990–996.
25. Silk TJ, Vance A, Rinehart N, et al. White-matter abnormalities in attention deficit hyperactivity disorder: a diffusion tensor imaging study. *Hum Brain Mapp* 2009; 30: 2757–2765.
 26. Voineskos AN, Farzan F, Barr MS, et al. The role of the corpus callosum in transcranial magnetic stimulation induced interhemispheric signal propagation. *Biol Psychiatry* 2010; 68: 825–831.
 27. Koenigs M and Grafman J. The functional neuroanatomy of depression: distinct roles for ventromedial and dorsolateral prefrontal cortex. *Behav Brain Res* 2009; 201: 239–243.
 28. Yang X, Zhang J, Lang L, et al. Assessment of cortical dysfunction in infantile esotropia using fMRI. *Eur J Ophthalmol* 2014; 24: 409–416.
 29. Catani M, Howard RJ, Pajevic S, et al. Virtual in vivo interactive dissection of white matter fasciculi in the human brain. *Neuroimage* 2002; 17: 77–94.
 30. Xiao JX, Xie S, Ye JT, et al. Detection of abnormal visual cortex in children with amblyopia by voxel-based morphometry. *Am J Ophthalmol* 2007; 143: 489–493.
 31. Gupta S, Kumaran SS, Saxena R, et al. BOLD fMRI and DTI in strabismic amblyopes following occlusion therapy. *Int Ophthalmol* 2016; 36: 557–568.
 32. Coenen VA, Panksepp J, Hurwitz TA, et al. Human medial forebrain bundle (MFB) and anterior thalamic radiation (ATR): imaging of two major subcortical pathways and the dynamic balance of opposite affects in understanding depression. *J Neuropsychiatry Clin Neurosci* 2012; 24: 223–236.
 33. Spalletta G, Fagioli S, Caltagirone C, et al. Brain microstructure of subclinical apathy phenomenology in healthy individuals. *Hum Brain Mapp* 2013; 34: 3193–3203.
 34. McBain HB, MacKenzie KA, Au C, et al. Factors associated with quality of life and mood in adults with strabismus. *Br J Ophthalmol* 2014; 98: 550–555.
 35. McBain HB, MacKenzie KA, Hancox J, et al. Does strabismus surgery improve quality and mood, and what factors influence this? *Eye (Lond)* 2016; 30: 656–667.
 36. Zheng Z, Xiao Z, Shi X, et al. White matter lesions in chronic migraine with medication overuse headache: a cross-sectional MRI study. *J Neurol* 2014; 261: 784–790.
 37. Qiu YW, Su HH, Lv XF, et al. Abnormal white matter integrity in chronic users of codeine-containing cough syrups: a tract-based spatial statistics study. *AJNR Am J Neuroradiol* 2015; 36: 50–56.